Microscopic Analysis of Aroma Chemical Distribution on Fibers. I. *cis*-3-Hexenyl Salicylate

Haiqing Liu,[1] S. Kay Obendorf,[1] Timothy J. Young,[2] Michael J. Incorvia[2]

[1]*Department of Textiles and Apparel, Cornell University, Ithaca, New York 14853*
[2]*International Flavors & Fragrances, 1515 State Highway 36, Union Beach, New Jersey 07335*

Received 3 June 2003; accepted 15 August 2003

ABSTRACT: The distribution of aroma chemical *cis*-3-hexenyl salicylate, on both longitudinal and cross-sectional fiber directions, was identified through backscattered electron microscopy and X-ray microanalysis including X-ray spectrum and X-ray map. Three fibers—cotton, lyocell, and polyester [poly(ethylene terephthalate) (PET)]—were used as substrates to evaluate the influence of fiber physical/chemical nature on the distribution of *cis*-3-hexenyl salicylate. It was found that the distribution of *cis*-3-hexenyl salicylate on the external and internal fiber surfaces correlated strongly with the chemical structure, roughness, and both pore and capillary structure of the textiles. *cis*-3-Hexenyl salicylate distributed through the whole cotton fiber cross section with higher concentrations in lumen and crenulations, whereas it distributed relatively uniformly in the surface and cross section of lyocell fiber. This is believed to relate to the macro- and micropores, macroscopic roughness, and the presence of a larger number of polar groups for these cellulose fibers. In contrast, *cis*-3-hexenyl salicylate accumulated at a few spots on the fiber surfaces of PET and in interfiber spaces of closely packed fibers, attributed to lower polarity, round cross-sectional shape, smooth surfaces, and fewer voids of the PET fiber structure. © 2004 Wiley Periodicals, Inc. J Appl Polym Sci 91: 3557–3564, 2004

Key words: aroma chemical; fibers; structure; morphology; voids

INTRODUCTION

Aroma chemical delivered through fabric care products is an important aspect of consumer satisfaction. Thus, the measurement of the physicochemical basis of aroma chemical performance has received much attention. Vapor pressure, odor perception limit, odor intensity, and water solubility are quantifiable parameters related to odor perception and substantivity.[1] Olfactometry, solid-phase microextraction (SPME), and gas chromatography/mass spectroscopy (GC/MS) methods are established methodologies to monitor the stability and substantivity of aroma chemicals on fabric. How an aroma chemical interacts with a fiber substrate is less well defined particularly at the microscopic level. This research focuses on defining the distribution of aroma chemical on and within fiber structures. The goal is to understand mechanisms of adsorption, retention, and distribution by investigating factors such as morphology, capillary structure, and chemistry of fibers.

Electron microscopy techniques have proven to be effective for the analyses of the distribution of chemical finishing agents and soils on fibers and within the yarn structure. These studies point out that the penetration and distribution of these materials are related strongly to the chemical and physical characteristic of the textile substrates.[2–8] Our work defines the distribution of aroma chemical on fiber surfaces using electron microscopy and X-ray microanalysis techniques.

In this study, unsaturated aroma compound *cis*-3-hexenyl salicylate was selected as a model aroma chemical for treating 100% cotton, lyocell, or polyester fabrics and applied from an alcohol solution by pipette. Osmium tetroxide reacts with the unsaturated aroma chemical providing a tag in the backscattered electron (BSE) imaging and X-ray analyses. Both longitudinal and cross-sectional fiber directions were analyzed to provide a detailed map of aroma chemical distribution on the fibers.

EXPERIMENTAL

Fabrics

Both bleached cotton print cloth style 400 and polyester (100% Dacron, type 54, style 777) were purchased from Testfabrics (West Pittston, PA). Lyocell (Tencel® Chambray) was from Courtaulds Inc. (Axis, AL). Before use, all three fabrics were rinsed by flowing tap water for 1 h, followed by washing with distilled water, air-dried at 23°C, and conditioned at 65 ± 2% relative humidity for at least 24 h.

These three fabrics with varied physiochemical characteristics, including molecular structure, surface

Correspondence to: S. Obendorf (sko3@cornell.edu).

Journal of Applied Polymer Science, Vol. 91, 3557–3564 (2004)

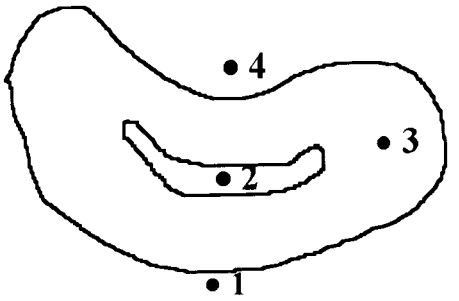

Figure 1 Morphological locations on the cotton fiber for collection of X-ray microanalysis data: (1) fiber surface, (2) lumen, (3) secondary wall, and (4) crenulation.

and internal morphology, capillary structure, and packing behavior, were used to study their effects on the distribution of aroma chemical on the fibers. Cotton print cloth is composed of natural cellulose fibers. As confirmed by scanning electron microscopy (SEM), transmission electron microscopy (TEM), and atomic force microscopy (AFM) techniques,[3–9] the surface of cotton fiber is far from smooth and regular. The shape of cotton fiber is commonly described as a "collapsed tube." There are distinct morphological regions in the cotton fibers (Fig. 1), including the external fiber surface, lumen, secondary wall, and crenulation (also know as V-groove). Lyocell, a microdenier fiber manufactured by solvent-spinning of cellulose, has the same molecular structure as that of cotton (linear polymer consisting of β-1,4-anhydroglucose repeating unit), but has no lumen and crenulation features; it has a round morphology with microfibrillar structure. Dry lyocell fibers have been reported to contain three phases: crystalline, larger air-filled voids, and smaller-defect regions that are formed during the solvent-spun manufacturing process. Diameters of the voids are in the range of 28–50 Å.[10] Polyester is a synthetic fiber of poly(ethylene terephthalate) (PET) with a round cross-sectional shape, manufactured by the melt-spinning method. PET fibers have very few or no voids and irregularities as documented by inverse gas chromatography experiments.[11]

Chemicals

Osmium tetroxide (2%) aqueous solution, and Spurr's low-viscosity resin kit were purchased from Electron Microscopy Sciences (Fort Washington, PA). *cis*-3-Hexenyl salicylate was supplied by International Flavors and Fragrances (Union Beach, NJ) and used as received.

Application method

A 0.2-mL aliquot of 1% (w/v) *cis*-3-hexenyl salicylate/EtOH solution was delivered by pipette onto one fabric swatch (Ø = 5 cm), followed by air-drying to allow the evaporation of ethanol. At time intervals of 10 min and 24 h, a small piece of each treated fabric was exposed to osmium tetroxide vapor for several hours in an enclosed container, to prepare the sample for microscopic analysis. Control cotton specimens were not treated with aroma chemical but were exposed to osmium tetroxide vapor. Theoretically, osmium tetroxide vapor does not react with cellulose or PET polymers because of the lack of unsaturated bonds or other reactive sites.

Fiber analysis

Osmium-treated warp yarns were embedded in Spurr's low-viscosity resin according to formulation: resin ERL 4206 (10 g), flexibilizer DER 736 (6 g), hardener NSA (26 g), and accelerator DMAE (0.4 g). Resin blocks were made in natural silicone standard embedding molds with dimensions of $14 \times 5 \times 4$ mm (length $\times$ width $\times$ depth) and 21 cavities, with one yarn in each cavity. The resin blocks were cured at 70°C for about 10 h. The blocks were trimmed into trapezoidal shape. Thick cross sections (5–10 μm) were cut using a glass knife on a Sorvall Ultra-microtome MT-1 (Newtown, CT).

Both longitudinal and cross-sectional specimens were mounted on carbon stubs using carbon tape. Before microscopic analysis, the specimens were carbon coated using an Edwards Auto 306 high-vacuum evaporator (Edwards High Vacuum International, Wilmington, MA).

Microscopic analysis

BES images were recorded on a JEOL 440 scanning electron microscope (LEO Electron Microscopy, Japan) in the Cornell Center for Materials Research. An accelerating voltage of 15 kV and a working distance of 20 mm were used. For X-ray maps and energy-dispersive X-ray (EDX) analyses along with BSE images, a JEOL Superprobe JXA-8900R WD/ED combined microanalyzer was used with the following instrumental conditions: accelerating voltage 5 kV, magnification $\times$1000, and probe current 9.0×10^{-8} A.

EDX analyses were used to investigate the relative concentrations of retained aroma chemical within the fiber structures. Using a magnification of $\times$2000 and 30 s counting time, data were collected for cotton specimens using the 1-μm spot probe at selected morphological locations (Fig. 1). A probe current of 3–3.3 $\times 10^{-8}$ A and accelerating voltage of 10 kV were used to ensure generation of strong X-ray signals. Net X-ray counts from Os were obtained using an energy range of 1.64–2.11 keV. This large energy range for the Os line was taken to simplify the subtraction of the background from X-ray intensity data. The intensity for the

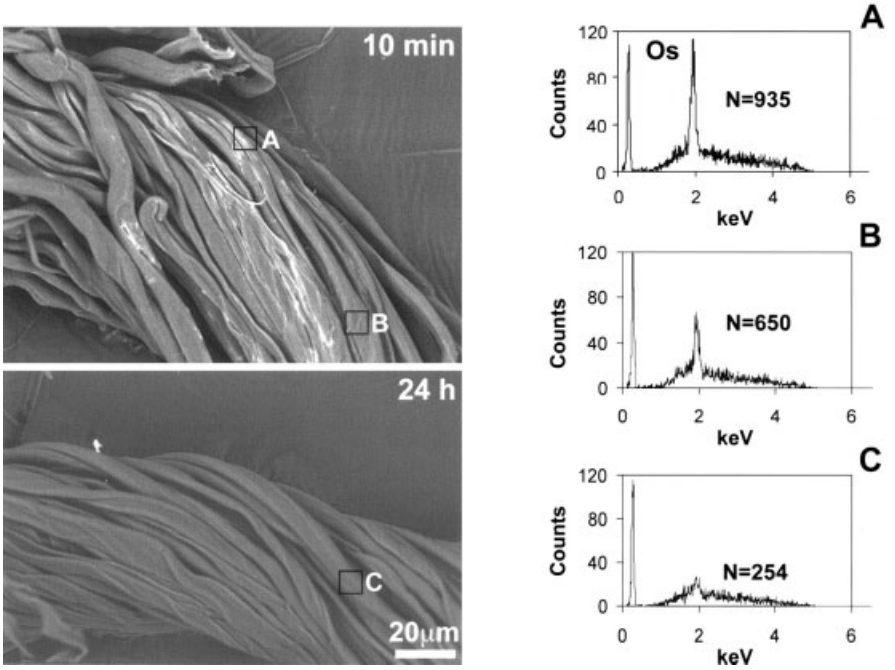

Figure 2 BSE and X-ray spectra of cotton treated with 1% *cis*-3-hexenyl salicylate, in air for 10 min and 24 h.

characteristic X-rays from Os was the net reading (i.e., the difference between gross count and background).

Interpretation of BSE and X-ray microanalysis

SEM imaging shows the topography of materials, whereas BSE imaging is sensitive to chemical composition of material as well as topography. For example, a heavy element like Os generates a higher intensity of backscattered electrons than lighter elements such as carbon, oxygen, and nitrogen. In our study, the bright areas in the BSE images indicate the locations of Os and thus the location of the aroma chemical. However, BSE imaging does not detect low concentration or uniform distributions of the heavy element on the fiber surfaces or cross sections. Therefore, it is also necessary to use EDX analysis to further define the distribution of aroma chemical in the fibers. By putting the X-ray spot probe on a location of interest for a selected time, X-ray net counts were obtained for the energy range of interest; analysis of these data allowed comparisons of aroma chemical distribution at various morphological locations.

For X-ray mapping, the spectrometer was tuned to a specific element or energy window of interest while the beam was scanned over the specimen. By this method, distribution maps of the selected element (Os) were produced. As the specimen area was scanned, all the pulses of the energy-dispersive detector that fall inside the selected energy interval were used to produce image intensity at the point corresponding to the position of the beam on the specimen. Concentration of the select element was indicated by the concentration of bright dots per unit area or by color-coding based on intensity. It is important to note that, because of the continuous background inside the selected energy windows, spurious bright dots can also be produced in regions not containing the element of interest. This is a serious problem for low concentrations. It is often necessary to spend 5 to 10 min to collect an adequate signal for a useful image.[12–14]

RESULTS AND DISCUSSION

Distribution of *cis*-3-hexenyl salicylate on cotton fiber surfaces

The distribution of *cis*-3-hexenyl salicylate from alcohol solution deposited by pipette on cotton fibers is heterogeneous and governed by surface roughness and capillary spacing of fibers (Fig. 2). High concentrations of aroma chemical appear in crevices and irregular morphological locations along fibers and within the yarn structure. After storing the treated fabric at ambient condition for 24 h, the high concentration areas were no longer present, suggesting release of aroma chemical from the fibers over time. Although no brightness differences were observed across the surfaces of the treated fibers after 24 h, it is not accurate to conclude that no aroma chemical remains on the fiber surfaces (i.e., those areas that appeared as dark monotone in the BSE image). In setting the microscope to obtain a quality image with accept-

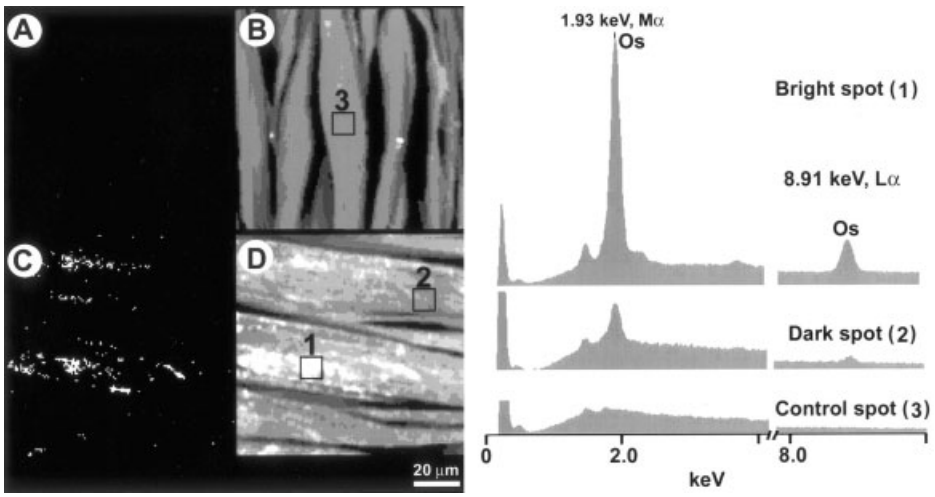

Figure 3 X-ray maps and BSE of control cotton (A, B), and cotton treated with 1% *cis*-3-hexenyl salicylate in air for 10 min and (C, D) X-ray spectra of corresponding spots.

able contrast, the brightness may be compromised. In our case, low concentrations of Os on the fiber surfaces did not produce strong enough signals to show brightness in the BSE image. Therefore, dark areas along the fiber implied either low or no content of Os, and thus small or no residual aroma chemical in that position.

X-ray microanalysis is more effective in providing detailed information on the chemical composition of material at low concentrations. Both X-ray spectra from bright and dark spots show obvious Os signal with different net counts, which acts as an indicator of relative concentration; higher net counts suggest higher content of Os (Fig. 2). In Figure 2, the marked bright spot had net counts of 935, and the net counts of dark spots in the same image amounted to 650. After storage at ambient condition for 24 h, a spot probe of the darker surface had very slight Os net counts of 254, showing the retention of trace amounts of aroma chemical on the fiber surface. Net X-ray counts were zero on the control cotton fiber surfaces (Fig. 3).

X-ray maps recorded for the Os signal provided further information about aroma chemical distribution on fibers that were linked to the BSE images. High and low aroma chemical *cis*-3-hexenyl salicylate concentrations can be distinguished easily as bright and dark areas at various locations along the treated and control fibers [Fig. 3(B), (D)]. Figure 3(A) and (C) are the X-ray maps of the same specimen region as that in the BSE images [Fig. 3(B), (D)]. In addition to the distribution of aroma chemical, the relative amounts of aroma chemical at different locations are represented by the concentration of bright dots in the map. Therefore, we conclude that aroma chemical *cis*-3-hexenyl salicylate was retained on cotton fiber surfaces with different concentrations at varied locations.

Compared to the X-ray map of the control cotton fiber [Fig. 3(A)], the treated fabric has large areas with higher Os concentrations [Fig. 3(C)]. Using spot-scan mode X-ray spectra, the relative intensities of characteristic X-ray were acquired at bright, dark, and control spots marked on the treated and control fibers in Figure 3. The intensity of the Os peak at 1.93 keV can be used to illustrate Os concentration differences at the three locations. Using this methodology, we found that the control cotton fiber has no detectable Os signal, whereas the aroma chemical–treated fibers had detectable amounts of Os at both bright and dark locations evaluated.

Because cotton fibers have extensive pore structures and internal surfaces,[15,16] it is important to know whether the aroma chemicals penetrate into the interior of the fiber. BSE images and X-ray mapping were applied to characterize cross-sectional specimens treated with *cis*-3-hexenyl salicylate (Fig. 4). BSE images of cross sections of the cotton fibers show the characteristic irregular morphological shape and nonuniform sizes of cotton fibers [Fig. 4(B), (D)]. Morphological locations [i.e., surface, secondary wall, lumen, and crenulation and interfiber spaces, as reported by Obendorf[4–8]] can be identified clearly. The continuous background inside the selected energy window caused a few bright dots for the control cotton sample [Fig. 4(A)]. However, for *cis*-3-hexenyl salicylate-treated cotton fiber [Fig. 4(C)], high concentrations of bright dots were observed in the X-ray map, indicating the retention of *cis*-3-hexenyl salicylate on cotton fiber. Those bright dots correlate with the bright areas in the BSE image [Fig. 4(D)], which are the locations of the crenulations and cotton fiber surfaces.

To further study the distribution of aroma chemical within the cotton fiber, X-ray microanalyses were performed on the control and treated fiber cross sections at morphological locations [i.e., surface, secondary wall, lumen, and crenulation (Fig. 5)]. To relatively

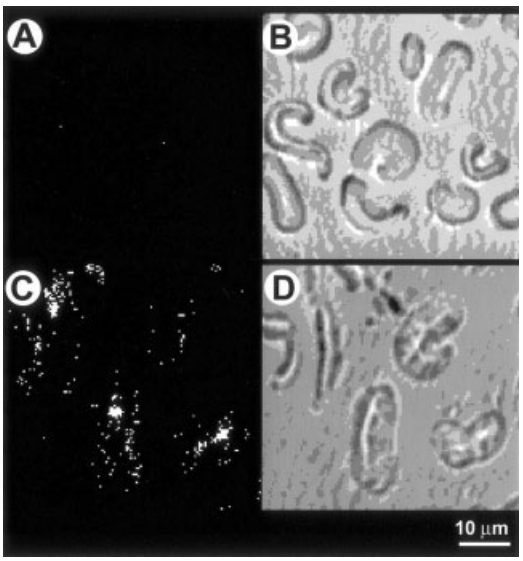

Figure 4 X-ray maps and BSE of cross section of control cotton (A, B) and cotton treated with 1% *cis*-3-hexenyl salicylate (C, D) in air for 10 min.

quantify the aroma chemical concentration entrapped at various locations on and within the fiber, 20 replications of X-ray net counts were made for each of four locations: fiber surface, lumen, crenulation, and secondary wall. Fibers were selected randomly from near the center of each yarn cross section and from near the yarn surface. Mean X-ray net counts at the selected morphological locations are shown in Figure 5. Standard deviation is shown as an error bar. All locations on the control cotton cross section show similar X-ray net counts of about 350, which is from the background signal. For cotton fibers treated with aroma chemical *cis*-3-hexenyl salicylate, X-ray net counts at each location were remarkably higher than the control. The crenulation of cotton fiber had the highest concentration of aroma chemical, whereas fiber surface, secondary wall, and lumen had similar concentrations of aroma chemical. These results are in good agreement with the observations shown in the BSE images (Fig. 4). In the process of applying aroma chemical solution on cotton fabric by pipette, capillary action is the driving force[9] for the spontaneous "flowlike" spreading (wicking) of aroma chemical solution in both warp and weft directions of cotton fabric. The liquid movement is expressed in the Lucas–Washburn equation:

$$dh/dt = r\gamma_{LV}cos\theta/4\eta h \quad (1)$$

where t is time; h is the length of the capillary; r is the capillary radius; η is viscosity; γ is the interfacial tension with LV meaning liquid and vapor, respectively; and θ is the contact angle.

Aroma chemical *cis*-3-hexenyl salicylate was deposited as a precipitate in the interfiber capillaries after the evaporation of solvent. The largest concentration of aroma chemical was observed in small surface grooves or crenulations. The crenulation acts as a microcontainer to hold aroma chemical solution. In addition, the evaporation rate heavily depends on air/surface interfacial area, for the same type and amount of aroma chemical; therefore, aroma chemical deposited on the fiber surface evaporates more readily than that in the crenulation, resulting in residual higher aroma chemical deposition in the crenulations.

Distribution of *cis*-3-hexenyl salicylate within cotton fibers

Transport of oily soils, chemical finishes, and detergents into the interior of cotton fibers has been well documented.[2–8] Cotton fibers have a characteristic microporous structure. Rowland et al.[15] defined pores in the cotton structure into which molecules with diameters greater than 16 Å can penetrate. Nelson and Oliver[16] found that the actual diameters of some pores are as large as 32–64 Å, which is 2–4 times the size of solutes. Small interfibrillar spaces of 12- to 50-Å width are present in the cotton fiber structure as well[17,18]; these spaces vary in size with the processing treatment of the fibers and the extent of swelling in water or other liquid media. These micropores and interfibrillar spaces greatly affect water uptake, dyeability, and washability.[7] Because the diameter of aroma chemical molecules is around 10 to 20 Å, they can be carried into those micropores and microspaces by the movement of the solvent and become deposited on surfaces internal to the cotton fiber. This phenomenon well explains our finding of aroma chemical *cis*-3-hexenyl salicylate in the interior of cotton fibers at locations such as the secondary wall and lumen.

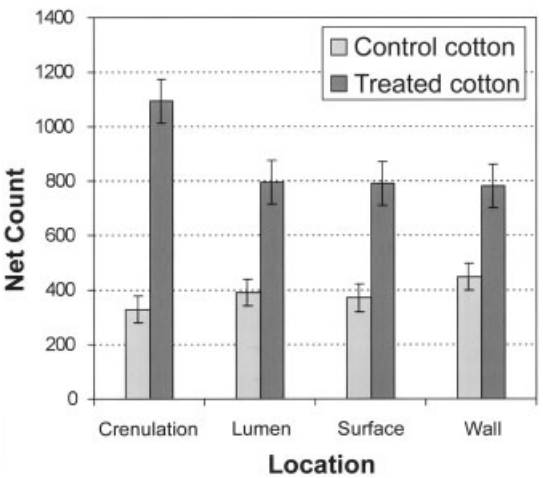

Figure 5 Relative concentrations of cis-3-hexenyl salicylate at various morphological locations on the cotton fiber as defined in Figure 1.

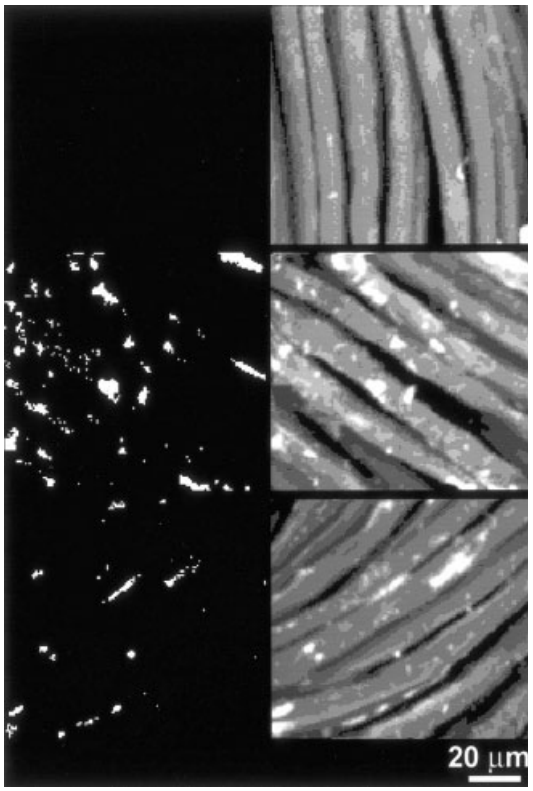

Figure 6 X-ray maps (left) and BSE (right) of control lyocell (top), lyocell treated with 1% *cis*-3-hexenyl salicylate, in air for 10 min (middle) and 24 h (bottom).

Effect of fiber morphology on distribution of aroma chemical

The round morphological shape of lyocell fibers can be compared to the twisted ribbon structure of cotton. Aroma chemical *cis*-3-hexenyl salicylate is more uniformly distributed over the surfaces of lyocell (Fig. 6) than over those of cotton fibers (Fig. 2). Differences in aroma chemical distribution are related to the different surface morphologies of these fibers. Crenulations on the cotton surface retain more aroma chemical than other locations, whereas the relatively smooth round surfaces of lyocell fibers have a more homogeneous distribution of aroma chemical over their surfaces. However, surface variations on lyocell also result in higher retention of aroma chemical as seen in some surface irregularities sites. Thus, we conclude that irregularities and defects along the fiber increase the retention of aroma chemical.

X-ray maps and BSE images show aroma chemical retained on the lyocell fiber surface as well as in the closely packed interfiber spaces (Fig. 6). The X-ray maps show aroma chemical was reduced or eliminated on lyocell fiber surfaces after 24-h storage at room temperature. For both cotton and lyocell fibers that are cellulose, we observed that fiber surface irregularities and defects affect aroma chemical distribution and that aroma chemical is lost from the surface over time because of evaporation.

The distribution of aroma chemical *cis*-3-hexenyl salicylate in the lyocell fiber cross sections is interesting (Fig. 7). No detectable signal appeared in the X-ray map of control lyocell, whereas *cis*-3-hexenyl salicylate distributed quite evenly throughout the lyocell fiber cross section. Produced by the solvent-spinning process, lyocell fibers contain small-defect regions and air-filled voids of sizes 28–50 Å.[10] Therefore, *cis*-3-hexenyl salicylate/EtOH solution penetrated into those voids and defect regions, with aroma chemical retained there after solvent evaporation.

Round polyester fibers (PET) that differ in chemical composition from cotton and lyocell were treated with aroma chemical *cis*-3-hexenyl salicylate for comparison. Figure 8 shows X-ray maps and BSE images of treated PET fibers. Again, higher concentrations of aroma chemical were retained at the irregularities on the fiber surfaces and in closely packed interfiber spaces. The appearance of the aroma chemical distribution is similar to that observed for lyocell, which is also a manufactured fiber. In the X-ray maps of PET, the nonuniform distribution of aroma chemical on fibers is visible. After 24 h, most retained aroma chemical is in the interfiber spaces. These interfiber spaces are small hydrophobic capillaries within the yarn structure formed by packing of PET fibers.

The distribution of aroma chemical on PET fiber cross sections is shown in Figure 9. No Os signal was observed in the X-rap map of control PET fiber, whereas high concentrations of *cis*-3-hexenyl salicylate are observed on some fiber surfaces particularly within interfiber spaces formed by closely packed fi-

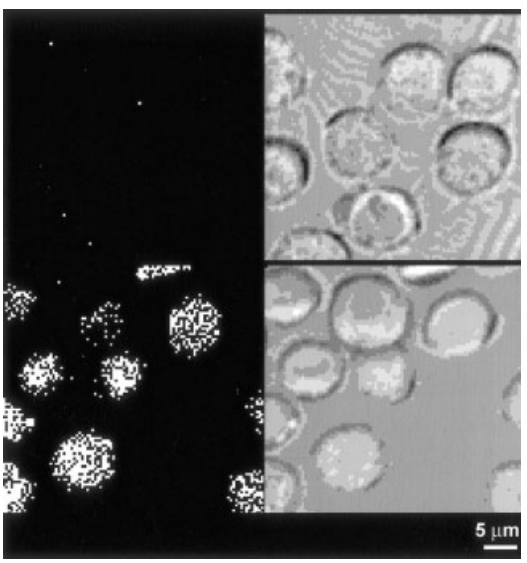

Figure 7 X-ray maps (left) and BSE (right) of cross section of control lyocell (top) and treated lyocell with 1% *cis*-3-hexenyl salicylate (bottom) in air for 10 min.

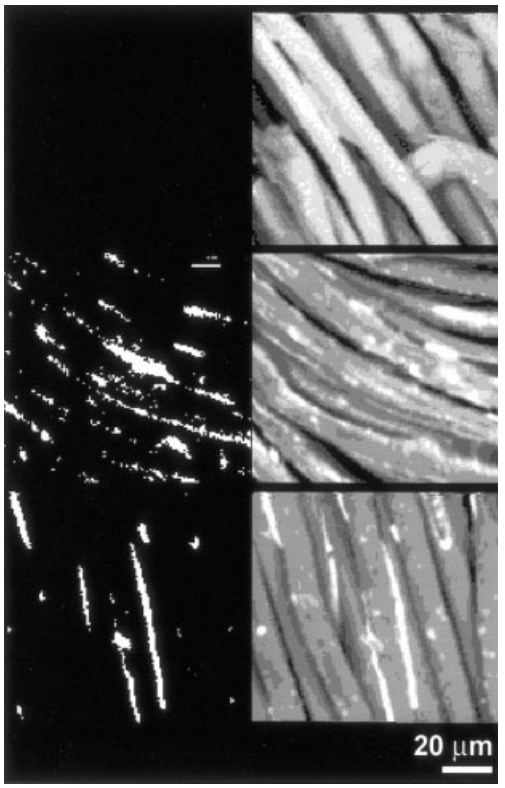

Figure 8 X-ray maps (left) and BSE (right) of control PET (top), PET treated with 1% *cis*-3-hexenyl salicylate, in air for 10 min (middle) and 24 h (bottom).

bers. No signal was observed for Os-tagged *cis*-3-hexenyl salicylate in the interior of the PET fibers, suggesting no *cis*-3-hexenyl salicylate/EtOH solution penetrated into the bulk of PET fiber. PET has a highly crystalline structure and low polarity, making it unlikely that *cis*-3-hexenyl salicylate is driven to the internal PET fiber structure by polar forces of the solvent. In addition, the treatment temperature of 20°C is well below the glass-transition temperature of PET (i.e., T_g = 70–80°C) obtained by DSC.[19] Thus, in our experimental condition there would be little movement of PET chain segments that might promote the entry of *cis*-3-hexenyl salicylate molecules into the amorphous regions. Because the PET structure has fewer voids and irregularities,[11] we would not expect to find *cis*-3-hexenyl salicylate on internal surfaces within the PET fiber.

We concluded that the morphological shape of fibers and their packing behavior have significant effects on the distribution of aroma chemical, *cis*-3-hexenyl salicylate. The irregularities and capillaries (e.g., crenulations on the cotton fiber) retain more aroma chemical than other morphological locations. Because of irregular shape and nonuniform fiber size as well as the specific yarn structure evaluated, the cotton fibers were packed loosely with larger interfiber spaces that did not hold aroma chemical deposits. However, because of the round shape and uniform size and the specific yarn structure, the lyocell and PET fibers were packed together tightly to form capillary structures that provided sites for aroma chemical accumulation.

Effect of chemical structure of fiber

The difference in the distribution of *cis*-3-hexenyl salicylate on the two cellulose fibers versus the PET fibers was striking. *cis*-3-Hexenyl salicylate was distributed through the whole fiber cross section for both cotton and lyocell on outer fiber surfaces and on internal surfaces (Figs. 4 and 7). However for PET fibers, we observed aroma chemical only on selected locations on PET fiber external surfaces and none on the interior of the fiber (Fig. 9).

Liquid wetting of a smooth solid surface is governed, in general, by the surface tensions (γ) of the liquid and solid. For a liquid to spread across a solid surface wetting the surface, the surface tension of the liquid (γ_l) must be less than that of the solid surface (γ_s). This theory is applicable to the distribution of *cis*-3-hexenyl salicylate in ethanol on fiber surfaces in our experiment. Surface tensions of cellulose, PET, ethanol, and *cis*-3-hexenyl salicylate are 42, 35, 22.8, and 61.6 mN/m at 20°C, respectively.[20] Based on theoretical principles, aroma chemical in ethanol solution will readily wet both cellulose and PET fiber surfaces because of the low surface tension of ethanol. However as a single component, *cis*-3-hexenyl salicylate would not be expected to spread over either cellulose or PET surfaces.

Because of the low surface tension of ethanol, we expect the *cis*-3-hexenyl salicylate/EtOH solution to

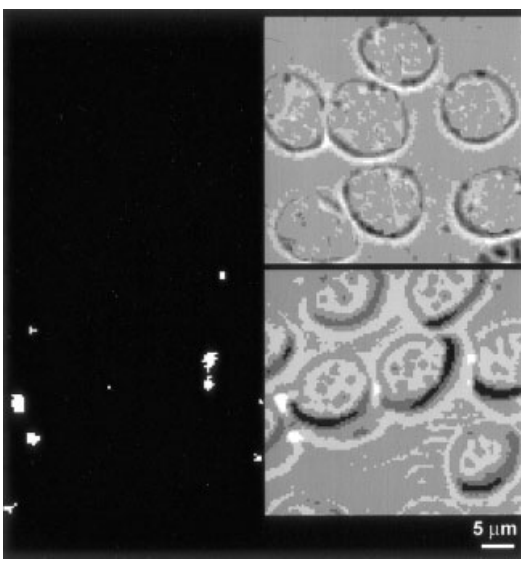

Figure 9 X-ray map and BSE of cross section of control PET (top) and PET treated with 1% *cis*-3-hexenyl salicylate (bottom), in air for 10 min.

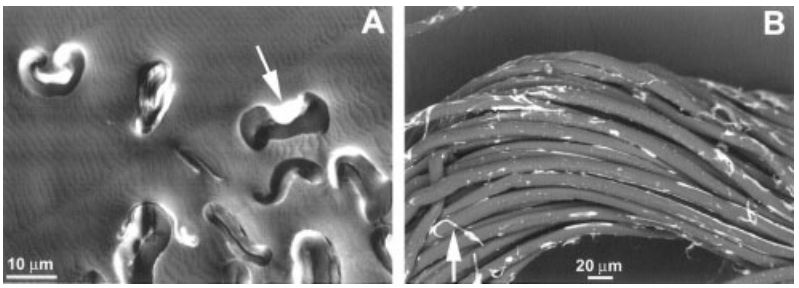

Figure 10 Distribution of *cis*-3-hexenyl salicylate on cotton cross section (A) and on lyocell (B).

spread across the fiber surfaces. *cis*-3-Hexenyl salicylate would be left behind on the fiber surface after the evaporation of ethanol. Self-retraction of liquid *cis*-3-hexenyl salicylate is predicted from the surface tension of the pure liquid. For PET fiber after evaporation of ethanol, it appeared that the residual liquid *cis*-3-hexenyl salicylate readily retracted to form spheres or small droplets on the fiber surface rather than spreading over the entire PET fiber surface. This behavior is consistent with theory, given that the surface tension of *cis*-3-hexenyl salicylate is much higher than that of PET. Retraction occurred easily on the round smooth surface and on the fiber with no or few voids and irregularities. This explanation is in accordance with our observation of the distribution of *cis*-3-hexenyl salicylate at only a few high concentration spots on the fiber surface (Fig. 9).

The *cis*-3-hexenyl salicylate/EtOH solution also spread across the fiber surfaces of the two cellulose fibers. However, we think that the liquid *cis*-3-hexenyl salicylate did not retract to form observable droplets as observed on PET fibers. Rather, it was retained in the irregularities on the fiber surfaces [Fig. 10(A)], on the microfibrils [Fig. 10(B)], in the micropores, and/or in the capillary structures. The high polarity of cellulose with large numbers of polar hydroxyl groups on the molecular chains also may act as a driving force for the penetration of *cis*-3-hexenyl salicylate into the pores and voids into the fibers. This would be consistent with the observed distribution of aroma chemical on cotton (Fig. 4) and lyocell (Fig. 7).

CONCLUSIONS

The combination of BSE image and X-ray mapping was used successfully to define the distribution of aroma chemical on fibers using osmium tetroxide tagging of C═C bonds in *cis*-3-hexenyl salicylate. The presence and relative concentration of aroma chemical *cis*-3-hexenyl salicylate in specific locations were evaluated using X-ray spectrum through recognizing the intensity of characteristic X-ray lines. Aroma chemical was retained and distributed over the entire fiber surface, with higher concentrations in surface irregularities and morphological structures such as the crenulation in cotton. Low amounts of aroma chemical were retained on internal surfaces within the cotton and lyocell fibers. The physicochemical nature of fiber plays an important role in the retention and distribution of aroma chemical. The micropores, tiny fibrils, and irregular locations retain higher concentrations of aroma chemical. The capillary structure formed by close packing of fiber such as observed for lyocell and PET fibers accumulated high concentrations of aroma chemical. Surface tension is an important factor affecting the residual distribution of *cis*-3-hexenyl salicylate, particularly on smoother PET fibers.

References

1. Stora, T.; Escher, S.; Morris, A. Chimia 2001, 55, 406.
2. Goynes, W. R.; Carra, J. H. Proc Ann Meet Electron Microsc Soc Am 1975, 33, 78.
3. Goynes, W. R.; Vigo, T. L.; Bruno, J. S. Text Res J 1990, 60, 277.
4. Obendorf, S. K. J Coated Fabrics 1983, 13, 24.
5. Obendorf, S. K.; Varanasi, A.; Mejldal, R.; Thellersen, M. J Surfact Deterg 2001, 4, 233.
6. Obendorf, S. K.; Mejldal, R.; Varanasi, A.; Thellerson, M. J Surfact Deterg 2001, 4, 43.
7. Obendorf, S. K.; Borsa, J. J Surfact Deterg 2001, 4, 247.
8. Obendorf, S. K.; Klemash, N. A. Text Res J 1982, 52, 434.
9. Shen, W.; Parker, I. H. J Colloid Interface Sci 2001, 240, 172.
10. Vickers, M. E.; Briggs, N. P.; Ibbett, R. N.; Payne, J. J.; Smith, S. B. Polymer 2001, 42, 8241.
11. Gozdz, A. S.; Weigmann, H. D. J Appl Polym Sci 1984, 29, 3965.
12. Benke, K. K.; Hedger, D. F. Eur J Phys 1991, 12, 175.
13. Smith, R. W. Microsc Today 2002, 5–6, September/October.
14. Lifshin, E. In: Scanning Electron Microscopy; Wells, O. C., Ed.; McGraw-Hill: New York, 1974; Chapter 10.
15. Rowland, S. P.; Wadeand, C. P.; Bertoniere, N. R. J Appl Polym Sci 1984, 29, 3349.
16. Nelson, R.; Oliver, D. W. J Polym Sci Part C 1971, 36, 305.
17. Haigler, C. H. In: Cellulose Chemistry and Its Applications; Nevell, T. P.; Zeronian, S. H., Eds.; Ellis Horwood: West Sussex, UK, 1985; p. 30.
18. Young, R. A. In: Cellulose Structure, Modification and Hydrolysis; Young, R. A.; Rowell, R. M., Eds.; Wiley: New York, 1986; p. 91.
19. Stinson, R. M.; Obendorf, S. K. J Appl Polym Sci 1996, 62, 2121.
20. Van Krevelen, D. W.; Hoftyzer, P. J., Properties of Polymer, Their Estimation and Correlation with Chemical Structure, 2nd ed.; Elsevier Scientific: London, 1976.